Molecular Interaction of Water Vapor and Air

Russell G. Wylie* and Robert S. Fisher

CSIRO Division of Applied Physics, National Measurement Laboratory, Lindfield, Australia 2070

The factor $f_w(T,p)$ by which air increases the saturation vapor pressure of water has been measured accurately for temperatures of 20, 50, and 75 °C and pressures to 14 MPa. An account is given of the measurements and of the analysis of the results to yield the interaction second virial coefficient $B_{aw}(T)$ and the first experimental values of the interaction third virial coefficient $C_{aaw}(T)$ of the vapor−gas mixture. When a Lennard-Jones potential is fitted, the three values of B_{aw} are found to be highly mutually consistent, allowing that coefficient and its derivatives to be calculated for a wide range of temperatures. The three values of C_{aaw} define the magnitude of this coefficient well for temperatures from about 0 to 100 °C, but for want of a reliable theoretical interpretation yield little information concerning its derivatives. The results for $B_{aw}(T)$ are compared with published experimental values, and those for both $B_{aw}(T)$ and $C_{aaw}(T)$ with published theoretical estimates. The work allows the vapor-pressure enhancement factor $f_w(T,p)$ and the vapor-concentration enhancement factor $g_w(T,p)$ to be calculated for a wide range of conditions, and substantially improves the accuracy with which the thermodynamic properties of the water−air system can be calculated.

Introduction

Vapor-Concentration and Vapor-Pressure Enhancement Factors for Saturated Water Vapor in Air. The presence of air at an elevated pressure substantially increases the concentration of water vapor in equilibrium with liquid water or ice as if the condensed phase were soluble in air. Components of the effect arise from the intermolecular forces in the gas mixture, the action of the pressure on the condensed phase (the Poynting effect), and the vapor-pressure lowering associated with the air dissolved in that phase (the Raoult effect). For a temperature of 20 °C and a pressure of 15 MPa, for example, the approximate contributions of these components are, respectively, an increase of 39%, an increase of 12%, and a decrease of 0.2%, while the whole effet is an increase of approximately 55%.

The vapor-concentration enhancement factor $g_w(T,p)$ may be defined by

$$c_w = g_w(T,p)c_w^o \tag{1}$$

where c_w is the saturation concentration in moles per unit volume of water vapor in air at the temperature T and total pressure p and c_w^o that of the pure vapor at the same temperature. Noting that the partial pressure p_w of the vapor is the product of the vapor mole fraction x_w and the total pressure, we may also define the vapor-pressure enhancement factor $f_w(T,p)$ by

$$p_w = f_w(T,p)p_w^o \tag{2}$$

where p_w^o is the saturation vapor pressure of pure water at T. Equation 2 is equivalent to

$$x_w = f_w p_w^o/p \tag{3}$$

It can easily be shown that

$$f_w = (Z/Z_w^o)g_w \tag{4}$$

where Z_w^o is the compressibility factor of the pure saturated vapor, and Z that of the saturated mixture. At elevated pressures the departures of g_w and f_w from unity are much greater than those of Z_w^o and Z, and so, in view of eq 4, are roughly equal. For instance, in the above numerical example, $Z_w^o = 0.999$, $Z = 1.001$, $g_w = 1.549$, and $f_w = 1.552$. Analogous enhancement factors g_i and f_i may be defined for air in equilibrium with ice.

The factor f_w is much more amenable to direct measurement and of much wider practical application than g_w. The reason is that f_w relates directly to the composition of the gas mixture, which remains constant when the gas flows through a system in which the temperature and pressure vary. Some direct applications of $f_w(T,p)$ are to the calculation of the composition of moist air from a humidity generator in which the gas is saturated over the liquid at a known temperature and pressure, the calculation of the temperature at which compressed air of a given water content will deposit liquid in tubing through which it flows, and the deduction of the composition of moist air from dew-point measurements made at an elevated pressure.

To measure f_w, a continuous stream of air may be saturated over liquid water at a measured temperature T and total pressure p and then expanded to a lower pressure at which its composition may be determined. Then f_w may be calculated from eq 3. The general method has been reviewed by Rowlinson and Richardson (1959) in the context of volatile solids, and by Mason and Spurling (1969).

Use of Virial and Interaction Virial Coefficients. We derive below an equation which expresses ln f_w as the sum of three parts which represent the intermolecular forces, the Poynting effect, and the Raoult effect. To obtain the first part, an expression for the partial thermodynamic potential of the water vapor in the gas mixture is obtained from the virial form of the equation of state for the mixture. This form is chosen because it has an exact statistical mechanical basis.

The general form of the virial equation of state has been derived by Mayer (1939). It can easily be shown to imply that, when one of the gases present is itself a mixture of constant composition, it is exact to treat that gas as a single component, not only in the equation of state but also in any thermodynamic formula. (In earlier work on the

0021-9568/96/1741-0133$12.00/0

present subject this proposition had been regarded as an assumption.) Thus, the parameters in that part of ln f_w which arises from the intermolecular forces are the virial coefficients for water vapor, those for air, and the interaction virial coefficients which correspond to groups of molecules containing at least one water molecule and one "air" molecule. Also, the concept of the intermolecular potential for the interaction of a water molecule and an air molecule has a precise meaning.

As the terms in ln f_w representing the Poynting and Raoult effects can be calculated with ample accuracy by substituting available property values in thermodynamic formulas, experimental data for f_w yield information concerning the part of ln f_w which contains the virial and interaction coefficients. In the present work, when available data for the virial coefficients and a sufficient estimate of one of the interaction coefficients are substituted, the experimental data for f_w yield data for $B_{aw}(T)$ and $C_{aaw}(T)$, which are, respectively, the interaction second virial coefficient corresponding to the interaction of a water molecule with an air molecule and the interaction third virial coefficient corresponding to the interaction of a water molecule with two air molecules. The coefficients B_{aw} and C_{aaw} together with those available from other sources form a complete set of second and third virial and interaction virial coefficients for moist air. Subject to limitations of accuracy, this set allows all the thermodynamic properties of the gas mixture to be calculated.

The Present Work. Extensive measurements of f_w for water in air have been made for temperatures of 20, 50, and 75 °C and pressures to 14 MPa. An early report on the project (Wylie and Fisher, 1974) described measurements for 20 and 50 °C, and the derivation of values of $B_{aw}(T)$. It also included a detailed proof that dry air may be treated as a single component. The air was atmospheric, and contained approximately 3 parts in 10^4 by volume of carbon dioxide. The value of 1.8 parts in 10^4 given in the early report is incorrect. In the following, the theory is outlined and the experiments and the analysis of the results are described. The resulting data for $B_{aw}(T)$ and its first and second derivatives, and those for $C_{aaw}(T)$ which are the first experimental data to be given for this coefficient, are the most accurate available. Some information can be deduced concerning the first derivative of $C_{aaw}(T)$, but very little concerning the second.

As the interaction between the dipole moment of a water molecule and the moment which this induces in an air molecule contributes to the intermolecular potential a term of the same form as that for the dispersion force, namely, an inverse sixth-power term, a Lennard-Jones (L-J) (6−m) potential is a good candidate to represent the whole interaction. As the two parameters of such a potential are determined by the values of B_{aw} for only two temperatures, the present results for three allow the consistency obtained with the potential to be tested. With an L-J (6−12), an L-J (6−18), or an L-J (6−24) potential, not only is a very high degree of consistency found, but practically the same values of B_{aw} are obtained on extrapolation to much lower or higher temperatures. An L-J (6−12) potential is fitted to the three results, and values of B_{aw} and its first and second derivatives are tabulated along with their uncertainties for temperatures from −100 to +200 °C. To predict reliably the temperature dependence of C_{aaw} is a complex problem. On the basis of a linear fit, this coefficient and its uncertainty are tabulated for temperatures from 0 to 100 °C.

The factors $g_w(T,p)$ and $f_w(T,p)$ and their uncertainties can be calculated with the aid of the derived values and uncertainties of $B_{aw}(T)$ and $C_{aaw}(T)$, correlations (considered below) which exist between the uncertainties in these values and that in the air−water−water interaction coefficient C_{aww} being taken into account. A skeleton table for temperatures from 0 to 100 °C and pressures to 15 MPa is given.

Experimental values of f_w, or of g_w from which f_w can easily be derived (eq 4), have been given in several publications (Wylie and Fisher, 1974; Pollitzer and Strebel, 1924; Goff and Gratch, 1945; Webster, 1950; Hyland and Wexler, 1973; Hyland, 1975). Values of $B_{aw}(T)$ have been given for the more accurate of these (Wylie and Fisher, 1974; Goff and Gratch, 1945; Hyland and Wexler, 1973), and some such values have been collated to give further values (Wexler *et al.*, 1981). All these essentially experimental values and two theoretical estimates (Mason and Monchick, 1965; Chaddock, 1965) are represented in a comparison with the present $B_{aw}(T)$ below. For $C_{aaw}(T)$, only a tenuous theoretical estimate (Mason and Monchick, 1965) is available for comparison.

Some results obtained with air containing nominally 1% by volume carbon dioxide will be published in a subsequent paper. They imply that the effect on f_w of the amount of carbon dioxide usually present in air (0.03−0.04% by volume) is negligible. Also, analogous measurements of f_w for water in pure oxygen have been made for temperatures of 25, 50, and 75 °C and pressures to 14 MPa. A relatively brief account of the results and their analysis will be published shortly.

Throughout the paper, the term "uncertainty", unless qualified, means the 3σ value obtained by summing the squares of its random and systematic parts. In the terminology developed by the International Organization for Standardization (ISO), the uncertainties quoted are *expanded uncertainties* obtained by multiplying the appropriately estimated standard deviations by a *coverage factor* of 3.

Theory

Derivation of the Equation for ln f_w. The partial thermodynamic potential of the water vapor in the gas mixture μ_w is equated to that of the water in the condensed phase μ_w^l, and the corresponding equation for pure water, $\mu_w^o = \mu_w^{l,o}$, is subtracted:

$$\mu_w - \mu_w^o = \mu_w^l - \mu_w^{l,o} \tag{5}$$

An expression for μ_w is derived from the virial equation of state of the gas mixture by calculating firstly the partial molar volume of the vapor and then integrating this with respect to the total pressure.

The equation of state may be written as

$$\frac{p\tilde{V}}{RT} = 1 + (B_{aa}x_a^2 + 2B_{aw}x_a x_w + B_{ww}x_w^2)/\tilde{V} + (C_{aaa}x_a^3 + 3C_{aaw}x_a^2 x_w + 3C_{aww}x_a x_w^2 + C_{www}x_w^3)/\tilde{V}^2 + \ldots \tag{6}$$

where $x_a = 1 - x_w$ is the mole fraction of air and $\tilde{V}$ is the molar volume of the mixture. The required expression for μ_w is found to be

$$\mu_w = \mu_w^\square + RT \ln[c_w RT/p^\square] + RTW \tag{7}$$

where $\mu_w^\square$ is the thermodynamic potential of pure water vapor in a hypothetical ideal-gas state at temperature T and pressure $p^\square$, and

$$W = \frac{2\beta}{\tilde{V}} + \frac{3}{2}\frac{\gamma}{\tilde{V}^2} + \frac{4}{3}\frac{\delta}{\tilde{V}^3} + \ldots \quad (8)$$

in which

$$\beta = B_{aw}x_a + B_{ww}x_w$$

$$\gamma = C_{aaw}x_a^2 + 2C_{aww}x_ax_w + C_{www}x_w^2 \quad (9)$$

$$\delta = D_{aaaw}x_a^3 + 3D_{aaww}x_a^2x_w + 3D_{awww}x_ax_w^2 + D_{wwww}x_w^3$$

and so on. To obtain μ_w^o, we simply take $x_a = 0$ in eq 9, and substitute c_w^o for c_w in eq 7.

For the condensed phase, we may calculate $\mu_w^l - \mu_w^{l,o}$ as the change in the potential which occurs when the pressure on pure liquid water is raised from the saturation vapor pressure to p, plus that which occurs when the appropriate amount of air dissolves in the liquid. The first part is $\int_{p_w^o}^{p} \tilde{V}_w^{l,o}\,dp$, where $\tilde{V}_w^{l,o}$ is the molar volume of the pure liquid. With the approximation that the dissolved air, of mole fraction x_a^l, forms an ideal solution, the marginally significant second part is $-RTx_a^l$.

Noting that eqs 1 and 4 give

$$RT\ln f_w = RT\ln(Z/Z_w^o) + RT\ln\left[\frac{c_wRT}{p^\square}\right] - RT\ln\left[\frac{c_w^oRT}{p^\square}\right] \quad (10)$$

we obtain on substituting in eq 5

$$\ln f_w = \ln(Z/Z_w^o) - (W - W^o) + \frac{1}{RT}\int_{p_w^o}^{p}\tilde{V}_w^{l,o}\,dp - x_a^l \quad (11)$$

where W^o is the value of W when $x_a = 0$. We then see from eq 4 that $\ln g_w$ is given by the right-hand side of eq 11 with the first term deleted.

Some Properties of the Equation for ln f_w. If the interaction virial coefficients and the terms for the Poynting and Raoult effects are taken equal to zero, eq 11 reduces to $f_w = Z/Z_w^o$. Thus, when hypothetically there is no interaction between the water and the air, it is g_w and not f_w which is unity.

As p tends to p_w^o, the terms in W which explicitly involve B_{ww} and C_{www} naturally tend to the corresponding terms in W^o. However, as $x_w/\tilde{V}$ varies with p only in proportion to g_w, these terms largely cancel at pressures as high as 3 MPa and substantially even at 14 MPa. Therefore, except at the highest pressures, the effect of B_{ww} and C_{www} on g_w is very small, and their effect on f_w occurs largely through the term $\ln(Z/Z_w^o)$. Further, except at very low pressures, Z is almost equal to the compressibility factor of dry air. Thus, the self virial coefficients adopted for the separate components must generate the compressibility factors of the components accuately rather than be true virial coefficients.

Ewald, Jepson, and Rowlinson (1953), and then other authors, have simplified eq 11 subject to $x_w \ll 1$. The only terms of W which they find remain are those in B_{aw}, C_{aaw}, D_{aaaw}, and so on. To show that the result is very misleading, we consider the ratio of the term in C_{aww} to that in B_{aw}:

$$\frac{\text{term in } C_{aww}}{\text{term in } B_{aw}} = \frac{3}{2}\frac{C_{aww}}{B_{aw}}f_w\left[\frac{p_w^o}{ZRT}\right] \quad (12)$$

If x_w is made small by lowering T, causing p_w^o and the ratio in eq 12 to diminish rapidly, the result is valid.

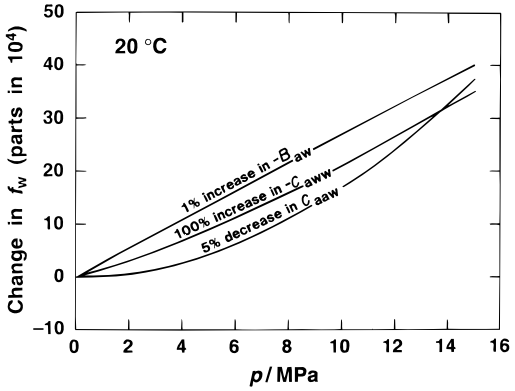

Figure 1. Changes in the f_w given by eq 11 for 20 °C and pressures up to 15 MPa for the indicated changes in B_{aw}, C_{aaw}, and C_{aww}.

However, if x_w is reduced by increasing the total pressure, as envisaged by the earlier authors, that ratio slowly *increases*, mainly through f_w, and the result is false. This can be seen also by comparing curves included in Figure 1 which, however, is given mainly to exemplify the magnitudes and trends of the interaction contributions to f_w.

As f_w is involved in x_w (see eq 3) and therefore in W and Z, it slightly affects the right-hand side of eq 11. However, f_w can easily be calculated from the equation by iteration.

Measurements

Outline of the Method. The principal parts of the apparatus are shown diagrammatically in Figure 2. A number of ancillary devices have been omitted from this. Dry compressed atmospheric air from a bank of high-pressure cylinders is passed first through a system in which it is very accurately equilibrated with liquid water at a precisely controlled and measured temperature and pressure. This system is essentially a precision humidity generator. The gas then passes into an analyzer in which the water vapor is absorbed (or in the earlier work, condensed in a low-temperature trap and subsequently transferred to absorption tubes) for weighing. The dry air is collected at a moderate pressure and also weighed. Then f_w is calculated from

$$f_w = \frac{m_w/M_w}{m_a/M_a + m_w/M_w}\left[\frac{p}{p_w^o(T)}\right] \quad (13)$$

where M_w and m_w are, respectively, the molecular weight and observed mass of the water and M_a and m_a the corresponding quantities for dry air.

Typically, with the gas flowing at the adopted nominal rate of 100 g/h, a single run occupies several hours, but much additional time is occupied in setting and stabilizing the conditions and carrying out the initial and final weighings. We now give some details of sections of the apparatus and the proving of their efficiencies, of the control and measurement of the temperature and pressure, and of the weighing of the water and air.

Saturator System. Gas enters the system from a bank of high-pressure gas cylinders through two pressure-reducing regulators and an adjustable low-resistance valve. It passes first through a heat-exchanger coil and a main saturator in which it bubbles through water in the interstices between glass beads. Then, in a "postsaturator", it flows through a bed of carborundum grits to remove any residual entrained spray and over wet surfaces where saturation is completed by transfer of the vapor. Finally, it passes through a pressure-reducing needle valve. The

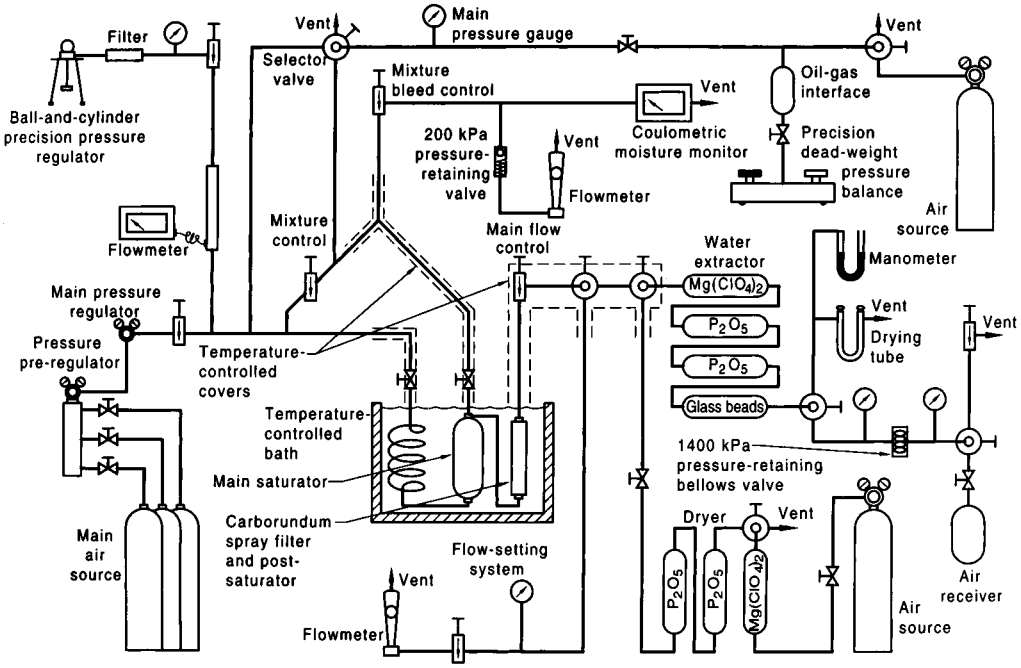

Figure 2. Diagram of the apparatus. A number of ancillary systems and components are not shown.

flow rate, which is not critical, is set by the needle valve and observed by diverting the output through a further valve to a flow meter at atmospheric pressure.

The whole saturator system is immersed in a water bath contained in a 14 L Dewar vessel of 200 mm internal diameter. For temperature control the bath contains also a specially designed resistance thermometer of very rapid response, an electrical wire heater and a closely associated heat-sink tube for work at 20 °C, and an impeller which circulates the water rapidly around a long vertical partition. Liquid can be circulated through the heat sink from an independent small refrigerated and temperature-controlled tank. Platinum resistance thermometers can be inserted. Outside, and close to the Dewar vessel, the gas-inlet tube is temperature-controlled by a small electronic unit, while all other tubes, electrical leads, and stems are brought out through a similarly temperature-controlled housing which covers the closure of the bath.

The vessel of the main saturator is a 1 L stainless-steel cylinder (Hoke, type HD1000). This is filled with glass beads 4.5 mm in diameter, and then about halfway with water (approximately 230 mL with the beads initially dry). The gas enters at the bottom through eight 3 mm holes in an inside ring-shaped tube. There are two outlet connections, one leading to the bottom of the postsaturator and the other to the pressure-measuring system.

The vessel of the postsaturator is a specially made stainless-steel cylinder 19 mm in internal diameter and about 180 mm long. In this, the gas passes first through a 35 mm deep bed of 60 mesh carborundum grits held between 400 mesh stainless-steel gauzes, and then through six parallel channels lined with white filter paper. The paper stands in an annular reservoir from which water (about 4 mL) rises 100 mm by capillarity to the top of the channels. Ancillary systems allow both the main saturator and the postsaturator to be charged with known quantities of water while under pressure, causing a minimum of disturbance.

Both pressure vessels are closed with Dowty seals, which are basically of stainless steel and present only a narrow ring of neoprene to the interior. Indeed, all valves and fittings in the saturator and analyzer systems are of type 316 stainless steel and are designed to avoid dead spaces. Tubing of the same steel, with a bright, smooth inside finish and of 4.8 mm outside and 3.4 mm inside diameter, is used throughout. The heat exchanger consists of a coil of 2.2 m of this. Before assembly, all components have been thoroughly cleaned, the last step being to pass steam, allowing the condensate to drain out.

During development of the main saturator the nature of the gas flow through the water between the beads, and the associated rise in water level, were studied using a full-scale glass model, and the mixing of the water (in relation to lateral heat transfer) was observed by making miniscule injections of a strong solution of potassium permanganate.

The principal impediment to temperature uniformity and a high efficiency of the system is the cooling as water evaporates into the incoming dry gas, but this has not been a difficult problem. The distribution of the temperature in the bath and over the saturator vessels was observed under normal operating conditions using multijunction thermocouples. No differences exceeding 1 mK were found.

To prove the efficiency of the main saturator, water-transfer runs were carried out without the postsaturator for progressively increased charges of water, commencing with the glass beads dry. The resulting approximately exponential plot of the saturation deficit shows that the adopted water charge is 4−5 times greater than necessary. Also, again without the postsaturator, water-transfer runs were carried out both with and without an additional saturator (at the same temperature) inserted before the heat exchanger. The results, for temperatures of 0−40 °C and pressures to 14 MPa, show that the saturation deficit is unlikely to exceed 0.2%.

It was shown using a small Wilson-type cloud chamber that, although the carborundum filter is associated with an entirely negligible drop in pressure, it removed all aerosol particles (condensation nuclei) from the gas. In considering the efficiency of the post saturator, we note that the carborundum filter must adsorb some water vapor. However, tests with a fast-responding hygrometer (Wylie, 1957) have shown that the effect is too rapid to be significant. A fiber-glass filter, on the other hand, hopelessly retards the attainment of equilibrium. We also note

that, on the bench, with evaporation to the atmosphere, capillarity raises water in the filter paper so that it has a glistening appearance at a height of at least 150 mm, and the vapor-pressure deficit corresponding to this water tension is only 7 parts in 10^6.

Rough calculations based on vapour transfer by diffusion alone show that the saturation deficit for the postsaturator is unlikely to exceed 0.3%. Thus, the deficit for the whole saturator system is estimated not to exceed 7 parts in 10^6 plus 0.3% of 0.2%, or 13 parts in 10^6, which is entirely negligible.

To provide an overall and ongoing test of the efficiency of both the saturator system and the water collection system, runs have occasionally been made for twice the normal flow rates. They have given results not differing significantly from those for the normal rates.

Measurement of the Saturator Temperature and Pressure. The temperature is controlled with a medium-term stability of 1 mK by means of an electronic proportioning controller. Utilizing the special fast-responding resistance thermometer and wire heater, and having the advantage of the rapid stirring, this corrects small disturbances in seconds. A continuous record of the temperature is provided by a platinum resistance thermometer connected to an automatic resistance bridge with an output to a chart recorder. Variations of 0.2 mK can easily be observed. Also, periodic measurements are made with an ITS-grade platinum resistance thermometer calibrated and used in conjunction with a premium NSL bridge (Thompson and Small, 1971).

It makes no significant difference whether the values of temperature in this paper are regarded as expressed on the IPTS-68 scale or the ITS-90 scale, the difference between which rises monotonically from zero at 0 °C to 26 mK at 100 °C (Preston-Thomas, 1990), but temperatures substituted in the adopted formulation for the saturation vapor pressure of water should be on the appropriate scale. The IPTS-68 has been used.

The uncertainty in the measured temperature is conservatively estimated to be 5 mK (systematic part 3 mK). However, it will be seen below that a constant small error in any one of the experimental temperatures simply produces an obvious offset in the corresponding values of ln f_w, which can be discounted.

The desired operating pressure is set and very accurately controlled by a dead-weight loaded ball-and-cylinder balance through which gas is bled from the input of the saturator system to the atmosphere. Originally developed for other purposes, the balance consists of a tungsten carbide ball seated on the plane end of a vertical thick-walled cylinder of nickel-maraging steel, the appropriate load being applied to the ball through a stirrup. The 19 mm ball and the plane square end and 12.7 mm bore of the cylinder were precision formed by lapping.

As the dew point of the gas from the main saturator is close to or above room temperature, a special device is necessary to avoid condensation in the pressure-measuring system. The pressure measurement tube from this vessel and another from the input to the saturator system and containing a small and adjustable flow resistance are taken to a common point from which gas is bled to the atmosphere at a slow rate. The humidity of the released gas is monitored with a CEC Coulometric hygrometer. The flow resistance is adjusted until the humidity indicates that the flows in the two legs are roughly equal. The pressure gauges and balance are connected to the leg containing dry gas, in which the pressure then very closely approximates that in the saturator.

The pressure is monitored with Wallace and Tiernan gauges of types FA233 and FA234 for pressures to 3.5 MPa, and a series of Heise test gauges from that pressure to 14 MPa. All have scales divided to 0.1% of full-scale deflection and are used only at high readings. Absolute pressure measurements are made with a Barnet Model V oil-type laboratory calibrator which has been calibrated at Bemetel-TNO and at NPL. The weights used with it have also been calibrated in our own laboratory. All necessary calibration and buoyancy corrections, including those associated with the gas−oil interface are, of course, applied. Atmospheric pressure is monitored with a Lambrecht barograph calibrated periodically with a Fortin barometer. The uncertainty in the measured absolute pressure is conservatively estimated to be 1 part in 10^4 at 1.5 MPa, declining to 0.5 part in 10^4 at 14 MPa, and to be about equally random and systematic.

Analyzer System. The pressure in this system is about 1.5 MPa. For the work at 20 and 50 °C the water was first condensed in a cold trap and then, at the end of a run, transferred slowly into conventional chemical absorption tubes. However, we will describe only the system developed to handle greater concentrations of water vapor which has been used for 75 °C and all subsequent work, including that with CO_2-doped air and that with oxygen. The two systems give the same results and uncertainty in m_w.

The water is absorbed directly in a train of four specially designed cylindrical glass vessels each of 32 mm inside diameter and 130 mL useful volume. The first is charged with anhydrous magnesium perchlorate, the next two with phosphorus pentoxide, and the fourth, used as a tare in weighing, partly with glass beads. Each tube is mounted within a close-fitting metal cylinder, the space between the glass and the metal being pressurized with gas to reduce the pressure difference across the glass to a low level.

The tubes are designed to be weighed on a 100 g balance by stringent classical procedures, their interiors accurately at atmospheric pressure. A buoyancy correction must be applied for the volume increase of the magnesium perchlorate on hydration. The predominant product appears to be the hexahydrate. With some doubt also about the densities of the anhydrate and hexahydrate (*Handbook of Chemistry and Physics*, 1991−2; *Handbook of Chemistry*, 1961), the volume occupied by the absorbed water has been taken to be (0.7 ± 0.2) cm^3/g, the corresponding correction to m_w being (0.084 ± 0.024)%.

The efficiency of the system is self-evident in that no significant increase in weight is observed in the third tube. The uncertainty in a measurement of m_w is estimated to comprise a random part of 0.16 mg and systematic part of $2.4 \times 10^{-4} m_w$.

The dry gas from the water extraction system is collected for weighing in a thin-walled stainless-steel aircraft breathing-oxygen cylinder of 35 L capacity and 8.3 kg tare weight. Two similar cylinders serve as tares in the weighing operations, in which buoyancy aspects are a major consideration. An allowance for an increase of approximately 60 mL in cylinder volume at the collection pressure (nominally 1.5 MPa) is marginally significant. The uncertainty in a measurement of m_a, which is on the order of 600 g, is estimated to consist of a random component of 2.5 parts in 10^4 and an approximately equal systematic component.

Results for f_w. Table 1 gives the results for f_w averaged for each set of conditions after adjusting the individual results to correspond accurately to the nominal conditions. The scatter of the so adjusted individual results may be seen in Figure 3, referred to further below.

Table 1. Experimental Values for the Vapor-Pressure (or Mole-Fraction) Enhancement Factor f_w for Water in Air[a]

p/MPa	t = 20 °C	t = 50 °C	t = 75 °C
1.4750	1.0467	1.0394	
2.1580			1.0514
3.5350	1.1144	1.0905	1.0799
7.0000	1.2356	1.1818	
7.3480			1.1668
10.1000	1.3532	1.2679	1.2247
14.0750	1.5135	1.3794	1.3165

[a] Each value is the mean of, on the average, six results.

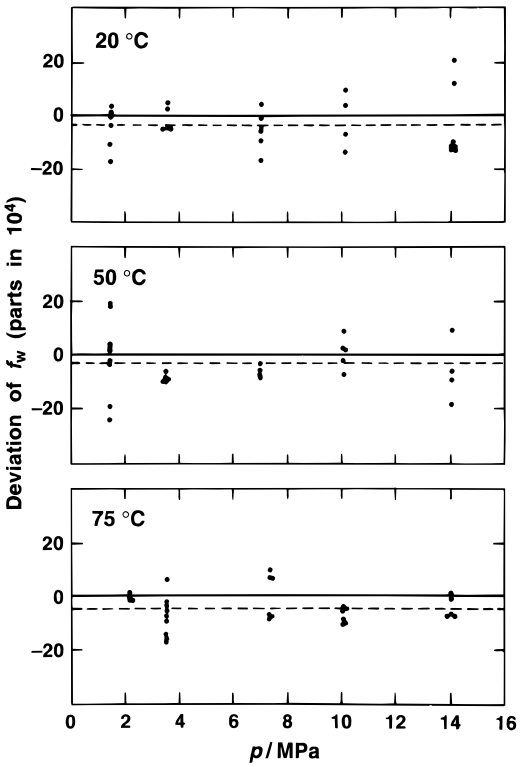

Figure 3. Deviations of the experimental values of f_w from the values given by eq 11 with B_{aw} and C_{aaw} fitted for each temperature (Table 2).

Property Values Substituted

To obtain f_w for each run from eq 13 and analyze the results using eq 11, we require data for M_a, M_w, $p_w^o(T)$, $B_{ww}(T)$, $C_{www}(T)$, $C_{aww}(T)$, $\tilde{V}_w^{l,o}(T,p)$, and $x_a^l(T,p)$, and also the properties of dry air needed to calculate $Z(T,p)$ and hence $\tilde{V}(T,p)$. Given by Harrison (1965), the molecular weight of dry air containing 3 parts in 10^4 by volume of carbon dioxide is 28.965 g/mol (C^{12} scale), and that of water 18.0153 g/mol. The corresponding gas constant is 8.3144 J K^{-1} mol^{-1}. For p_w^o we have adopted the formulation of Wexler (1976), with an uncertainty not exceeding 1 part in 10^4 for temperatures from 0 to 100 °C.

Primarily, B_{ww} and C_{www} must accurately reproduce the compressibility factor Z_w^o. The data of Wexler *et al.* (1981) and those of Goff (1949) give the same Z_w^o within 2 parts in 10^5 at 20 °C, 5 parts in 10^5 at 50 °C, and 1 part in 10^5 at 75 °C, and are equivalent for the present purposes. For temperatures from 0 to 100 °C, the estimated uncertainty in Z_w^o is 4 parts in 10^4. For C_{aww} there is no alternative to the theoretical estimate of Hyland and Mason (1975), with an indicated uncertainty of 200%.

The molar volume $\tilde{V}_w^{l,o}(T,p)$ of pure liquid water is taken from Kell (1975) and Kell and Whalley (1965). The first reference gives the volume at standard atmospheric pressure, and the second the volume for other pressures relative to that. The uncertainty is negligible. The mole fraction x_a^l of the dissolved air is the sum of the mole fractions of dissolved nitrogen, oxygen, and argon. We may lump the argon (about 0.9%) with the oxygen, as these gases have rather similar intermolecular forces, and then take the partial pressures of the oxygen and nitrogen in the gas to be $0.22p$ and $0.78p$, respectively. The low-pressure solubilities have been given as a function of temperature by Himmelblau (1960). Zoss *et al.* (1954) have shown that in the present range the solubility of oxygen is proportional to its partial pressure. The solubility of nitrogen, however, is proportional for only about 10% of the range. From the results of Wiebe *et al.* (1933) we deduce the adequate approximation that the nonlinearity is independent of the temperature, and represent it by a factor of $1 - 1.03 \times 10^{-2} p_n$/MPa, where p_n is the partial pressure of the nitrogen. There is no alternative but to regard the solubilities of the two components as additive. However, x_a^l is only marginally significant, its greatest value in the present work being 0.0019 which occurs for 20 °C and 14 MPa.

To calculate Z ($=P\tilde{V}/RT$), we require firstly all the virial and interaction coefficients of eq 6. Our source of B_{ww} and C_{www} has been given above, and B_{aw} and C_{aaw} are products of the present work (an iteration being implied). However, the self virial coefficients of dry air cannot be truncated after the third. The PVT data of Michels *et al.* (1954), which are undoubtedly more accurate than those of Holborn and Otto (1925), have been adopted. Z has been expressed as a polynomial in $\tilde{V}^{-1}$ which extends to the term in $\tilde{V}^{-7}$. Only the coefficients of the first two terms approximate true virial coefficients, but all the coefficients have been treated as such. The resulting Z is accurate at low pressures, where only the terms in $\tilde{V}^{-1}$ and $\tilde{V}^{-2}$ are significant. It is also accurate at high pressures, where terms containing x_w are negligible and it becomes simply the compressibility factor for dry air. It can further be shown to be accurate in the transition region.

The Michels results for air already include data for 50 and 75 °C. Values of the seven polynomial coefficients for 20 °C have been obtained by Bessel's interpolations of coefficients derived from the Michels data for 0, 25, 50, and 75 °C. For the present temperatures the uncertainty in Z, and hence that in $\tilde{V}$, is estimated to rise in proportion to the pressure to 10 parts in 10^4 at 14 MPa.

Derivation of B_{aw} and C_{aaw}

Values of B_{aw} and C_{aaw} for the Experimental Temperatures. The changes in the calculated ln f_w for increments in the B_{aw} and C_{aaw} substituted in eq 11 are almost proportional to p and p^2, respectively. Thus, when for a given temperature, approximate values of those coefficients are substituted, and the differences of the calculated values of ln f_w from the experimental values are least-squares-fitted by a quadratic polynomial in p, the coefficients of p and p^2 give adjustments which should be made to B_{aw} and C_{aaw}. A single iteration is likely to be adequate. The constant term obtained in the fit, which we denote by a, ideally should be zero, but inevitably a small nonzero value is found. As well as giving a, B_{aw}, and C_{aaw}, the final least-squares fit gives their random uncertainties and the correlations between them.

The values found for a, B_{aw}, and C_{aaw}, and for their random, systematic and total uncertainties, are given in Table 2. The deviations for the final fits are as plotted in Figure 3. For each temperature, the random uncertainty

Table 2. Values of a, B_{aw}, and C_{aaw} and Their 3σ Uncertainties for the Experimental Temperatures

		$10^4 \times$ uncertainty				uncertainty/(cm^3/mol)				uncertainty/(cm^3/mol)^2		
t/°C	10^4a	rand	syst	total	B_{aw}/(cm^3/mol)	rand	syst	total	C_{aaw}/(cm^3/mol)^2	rand	syst	total
20	−4	15	6	16	−32.39	0.59	0.38	0.70	1302	119	42	126
50	−3	16	6	17	−24.31	0.79	0.99	1.27	1348	200	80	220
75	−5	14	6	15	−18.67	0.64	1.85	1.96	1263	154	112	191

in $-B_{aw}$ is positively correlated with that in C_{aaw} with a correlation coefficient of 0.98. The random uncertainties for the different temperatures are, of course, uncorrelated. Conservatively, the systematic uncertainties for the different temperatures are regarded as fully correlated.

The systematic uncertainties in a, B_{aw}, and C_{aaw} are the statistical sums of the uncertainties in eq 11 which are, respectively, independent of p, proportional to p, and proportional to p^2. For a, contributions arise mainly from Z^o_w, m_w, m_a, and $p^o_w(T)$ through the measurement of T. Possible contributions from a small departure of the air from the accepted composition (affecting mainly M_a) and the release of adsorbed air from the porous magnesium perchlorate when it is hydrated cannot be estimated and have been neglected (but see next paragraph). For B_{aw}, the main contribution is from C_{aww}, while a contribution roughly 10 times smaller arises from Z. For C_{aaw}, a dominant contribution arises from C_{aww}. The contributions from this coefficient are easily calculated because the dependence of the C_{aww} term on the pressure can be resolved without significant residue into a component proportional to p and one proportional to p^2 by least-squares fitting.

That a, which varies surprisingly little from temperature to temperature, is smaller than even its systematic uncertainty (6×10^{-4}) testifies to the high absolute accuracy of the work. However, it will be seen below that its value has no effect on the values of B_{aw}, C_{aaw}, g_w, and f_w derived.

Values of B_{aw} and Its Derivatives for a Range of Temperatures. The two parameters of a Lennard-Jones potential can readily be derived from the values of B_{aw} for two temperatures using formulas given, for example, by Hirschfelder *et al.* (1964). To interpolate and extrapolate our data for $B_{aw}(T)$, we use a least-squares method to fit an L-J (6−12) potential to our values for three temperatures. (It makes little difference whether we work with the deviations of B_{aw} or those of f_w.) In the notation of Hirschfelder *et al.*, the result is

$$\epsilon/k = 140.67 \text{ K}$$

$$b_o = 57.61 \text{ cm}^3/\text{mol} \qquad (14)$$

Corresponding values of B_{aw}, $T(dB_{aw}/dT)$, and $T^2(d^2B_{aw}/dT^2)$ and their uncertainties are given in Table 3 for temperatures of −100 to +200 °C. The deviations of the experimental B_{aw} for 20, 50, and 75 °C are, respectively, only 0.01, −0.04, and 0.05 cm^3/mol, much smaller than even the corresponding random uncertainties of 0.59, 0.79, and 0.64 cm^3/mol.

When an L-J (6−18) or an L-J (6−24) potential is fitted instead, the changes in Table 3 are negligible except at the lowest temperatures. Even with the latter potential, the change in B_{aw} at −50 °C is only −0.7 cm^3/mol compared with an uncertainty of 3.4 cm^3/mol, and at −100 °C only −3.8 cm^3/mol compared with 7.6 cm^3/mol. This insensitivity to the form of the potential accords with the similar property for pure substances (Maitland *et al.*, 1981; Rowlinson *et al.*, 1954).

Treatment of the Results for C_{aaw}. A reliable theoretical interpolation of $C_{aaw}(T)$ would be a major undertaking, especially as a polar molecule is involved. Without it, the data (Table 2) warrant no more than a weighted linear least-squares fit. This gives the equation

$$C_{aaw}(T)/(\text{cm}^3/\text{mol})^2 = 1320 - 0.47t/°\text{C} \qquad (15)$$

Its relationship to the experimental points may be seen in Figure 6.

On a wide scale, the $C_{aaw}(T)$ curve must have a maximum at which C_{aaw} is positive, below which it falls with rapid acceleration to negative values, and above which it passes through an inflexion and then asymptotically approaches zero. Our experimental range clearly does not lie at temperatures below the maximum, and with extrapolation to lower temperatures the uncertainty must soon increase rapidly.

Values of C_{aaw} obtained from eq 15 for temperatures from 0 to 100 °C are given with their uncertainties in Table 4. In addition to random and systematic components of uncertainty arising from those in the three fitted values (Table 2), the uncertainties in Table 4 include an estimated statistically independent component to allow for our limited knowledge of the true shape of the $C_{aaw}(T)$ curve in the relevant temperature range. This amounts, respectively, to 10, 55, and 25 (cm^3/mol)^2 at 20, 50, and 75 °C, and increases to 100 (cm^3/mol)^2 at 0 °C and 75 (cm^3/mol)^2 at 100 °C.

Correlations of the Uncertainties in B_{aw} and C_{aaw}. When values of B_{aw} and C_{aaw} are obtained for an arbitrary temperature to calculate g_w or f_w, it is necessary to know the correlations between their uncertainties, and between those uncertainties and that of C_{aww}, to calculate the uncertainty in the result. The random uncertainties in values of B_{aw} and C_{aaw} for such a temperature do not have the almost 100% correlation of those in Table 2. That in B_{aw} has three components attributable to those of the three values in that table. Similarly, the systematic uncertainty has three components. The random and systematic uncertainties in C_{aaw} each has the analogous three components, but in addition C_{aaw} has the component which allows for the uncertainty concerning the shape of the C_{aaw} curve. Random components in B_{aw} and C_{aaw} which arise from measurements at different temperatures are uncorrelated, but those which relate to the same temperature are practically 100% correlated.

As all the systematic uncertainties in Table 2 arise very largely from the uncertainty in C_{aww}, the error in which may be regarded as roughly constant over the present temperature range, there are six systematic components of uncertainty in B_{aw} and C_{aaw} which are regarded as practically 100% correlated with one another and with the uncertainty in C_{aww}. The shape component in C_{aaw} is statistically independent.

Calculations of g_w and f_w

From eqs 11 and 4 we have

$$\ln g_w = -(W - W^o) + \frac{1}{RT}\int_{p^o_w}^{p} \tilde{V}^{l,o}_w \, dp - x^l_a \qquad (16)$$

Regardless of the errors in the property values substituted,

Table 3. Values of 3σ Uncertainties of B_{aw}, $T(dB_{aw}/dT)$, and $T^2(d^2B_{aw}/dT^2)$ for Temperatures from −100 to +200 °C

t/°C	B_{aw}/ (cm^3/mol)	uncertainty/ (cm^3/mol)	$T(dB_{aw}/dT)$/ (cm^3/mol)	uncertainty/ (cm^3/mol)	$T^2(d^2B_{aw}/dT^2)$/ (cm^3/mol)	uncertainty/ (cm^3/mol)
−100	−101.0	7.6	185.1	19.2	−461	40
−90	−91.0	6.6	170.4	18.1	−420	38
−80	−82.3	5.6	157.7	17.0	−385	36
−70	−74.6	4.8	146.7	16.1	−355	34
−60	−67.8	4.1	137.1	15.2	−330	33
−50	−61.7	3.4	128.6	14.5	−307	31
−40	−56.2	2.8	121.1	13.7	−288	30
−30	−51.3	2.2	114.3	13.1	−270	28
−20	−46.81	1.76	108.2	12.5	−255	27
−10	−42.72	1.33	102.7	11.9	−241	26
0	−38.99	0.98	97.7	11.4	−228	25
5	−37.24	0.84	95.3	11.2	−222	24
10	−35.56	0.74	93.1	10.9	−217	24
15	−33.95	0.68	91.0	10.7	−212	24
20	−32.40	0.67	88.9	10.5	−207	23
25	−30.91	0.71	86.9	10.3	−202	23
30	−29.48	0.78	85.1	10.1	−197	22
35	−28.11	0.88	83.2	9.9	−193	22
40	−26.78	0.99	81.5	9.7	−189	21
45	−25.50	1.10	79.8	9.5	−185	21
50	−24.27	1.22	78.2	9.3	−181	21
55	−23.08	1.34	76.6	9.2	−177	20
60	−21.94	1.46	75.1	9.0	−173	20
65	−20.83	1.58	73.7	8.8	−170	20
70	−19.76	1.70	72.3	8.7	−166.5	19.3
75	−18.72	1.82	71.0	8.5	−163.3	19.0
80	−17.72	1.93	69.7	8.4	−160.2	18.7
85	−16.8	2.0	68.4	8.2	−157.2	18.4
90	−15.8	2.1	67.2	8.1	−154.3	18.1
95	−14.9	2.3	66.0	8.0	−151.5	17.8
100	−14.0	2.4	64.8	7.8	−148.9	17.6
110	−12.3	2.5	62.7	7.6	−143.8	17.0
120	−10.7	2.7	60.6	7.3	−139.0	16.5
130	−9.2	2.9	58.7	7.1	−134.5	16.1
140	−7.8	3.1	56.8	6.9	−130.2	15.6
150	−6.5	3.2	55.1	6.7	−126.3	15.2
160	−5.2	3.4	53.5	6.5	−122.5	14.8
170	−4.0	3.5	51.9	6.3	−118.9	14.4
180	−2.9	3.7	50.5	6.1	−115.6	14.6
190	−1.8	3.8	49.1	5.9	−112.4	13.7
200	−0.8	3.9	47.7	5.8	−109.4	13.6

Table 4. Values and 3σ Uncertainties of C_{aaw} for Temperatures from 0 to 100 °C

t/°C	C_{aaw}/ (cm^3/mol)^2	uncertainty/ (cm^3/mol)^2	t/°C	C_{aaw}/ (cm^3/mol)^2	uncertainty/ (cm^3/mol)^2
0	1320	200	60	1290	150
10	1320	150	70	1290	170
20	1310	120	80	1280	200
30	1310	110	90	1280	230
40	1300	120	100	1270	270
50	1300	130			

every term in eq 16 tends to zero (and g_w approaches unity) as p is decreased to p^o_w. There is, therefore, no question of including the offset a, or any part of it, in the equation. Thus g_w and its uncertainty may be calculated directly from eq 16. The random uncertainty in g_w arises from B_{aw} and C_{aaw}, the six contributions from which are correlated as described above. The systematic uncertainty arises largely from B_{aw}, C_{aaw}, and C_{aww}, the correlations involved also having been already described.

Having thus obtained g_w and its uncertainty, we obtain f_w by multiplying g_w by Z/Z^o_w, and derive its uncertainty by statistically deleting the uncertainty in Z, which largely cancels with the uncertainty allowed for Z in the analysis which leads to Table 2, and statistically adding-in the uncertainty in Z^o_w, which was discarded in the analysis when a was taken equal to zero.

For a wide range of relatively low total pressures, the uncertainty in Z^o_w, which is independent of the pressure, is important. Thus, for 20 °C and atmospheric pressure, for example, the total uncertainty in g_w (=1.003 37) is only 0.5 part in 10^4 but that in f_w (=1.0042) is practically the same as in Z^o_w, i.e., 4 parts in 10^4. For a range of conditions, Wexler *et al.* (1981) erroneously assign to f_w an uncertainty well below that which they recognize for Z^o_w.

The averaged experimental values of f_w (Table 1) may be compared with values calculated from eq 11, B_{aw} being obtained from eq 14, or equivalently Table 3, and C_{aaw} from eq 15, equivalently Table 4. For the fifteen sets of conditions, the rms difference is found to be 8 parts in 10^4. If a is added to the experimental values, this is reduced to 6 parts in 10^4. Almost half of each rms difference is contributed by the point for 50 °C and 14 MPa, and is associated with the greater deviation of C_{aaw} for that temperature seen in Figure 6.

A skeleton table of values of g_w and f_w and their uncertainties is given for temperatures from 0 to 100 °C and pressures to 15 MPa in Table 5.

Discussion

Comparison with Earlier Work. At NBS, Hyland and Wexler (1973) made 5 measurements of f_w for 30 °C, 5 for 40 °C, and 17 for 50 °C. Hyland (1975) later supplemented these with one measurement for −20 °C, two for −10 °C, and four for 70 °C, and then collated all the corresponding values of $B_{aw}(T)$. (Only four of the NBS measurements are for pressures above 5 MPa.) The present $B_{aw}(T)$ is plotted in Figure 4 with Hyland's collated values, the experimental results of Goff and co-workers (1945), and the theoretical

Table 5. Values of g_w and f_w for Various Temperatures and Pressures[a]

t/°C	p/MPa = 0.1	p/MPa = 1	p/MPa = 2	p/MPa = 5	p/MPa = 10	p/MPa = 15
0	1.00420, 0.9	1.0428, 9	1.0870, 17	1.2272, 37	1.4794, 63	1.7397, 98
	1.00412, 4.1	1.0376, 9	1.0761, 17	1.2003, 37	1.4361, 63	1.7053, 98
20	1.00333, 0.5	1.0343, 5	1.0694, 8	1.1778, 16	1.3642, 18	1.5489, 20
	1.00417, 4.0	1.0321, 6	1.0640, 9	1.1648, 16	1.3494, 18	1.5524, 20
40	1.00258, 0.3	1.0278, 3	1.0560, 6	1.1417, 14	1.2842, 22	1.4209, 32
	1.00482, 4.0	1.0287, 5	1.0555, 7	1.1393, 14	1.2889, 22	1.4488, 32
60	1.00184, 0.3	1.0226, 4	1.0457, 7	1.1147, 15	1.2267, 25	1.3317, 35
	1.00580, 4.0	1.0271, 6	1.0503, 8	1.1215, 15	1.2462, 25	1.3770, 35
80	1.00102, 0.3	1.0184, 5	1.0376, 9	1.0944, 21	1.1849, 34	1.2682, 45
	1.00566, 4.0	1.0274, 6	1.0479, 10	1.1101, 21	1.2172, 34	1.3278, 45
100		1.0147, 7	1.0309, 14	1.0786, 34	1.1535, 64	1.2216, 93
		1.0292, 8	1.0481, 14	1.1039, 34	1.1985, 64	1.2948, 93

[a] Upper values, g_w; lower values, f_w. Uncertainities (3σ) are parts in 10^4.

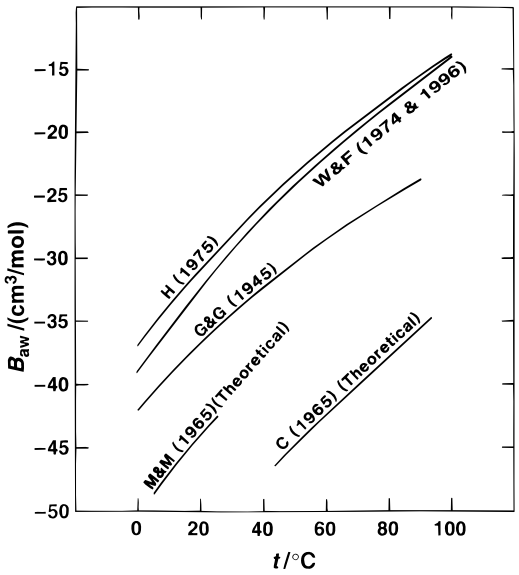

Figure 4. $B_{aw}(T)$ for the present work and earlier work: C, Chaddock (1965); G&G, Goff and Gratch (1945); H, Hyland (1975); W&F, Wylie and Fisher (1974 and the present work).

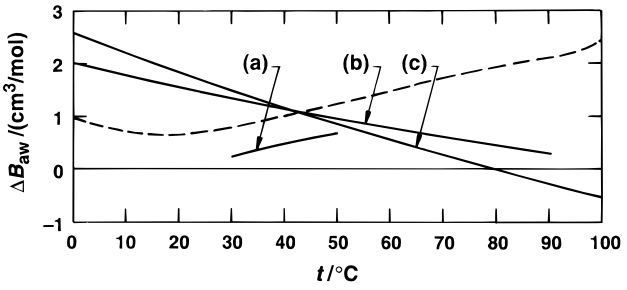

Figure 5. Differences of the NBS data for B_{aw} from the present data: (a) Hyland and Wexler (1973); (b) Hyland (1975); (c) Wexler *et al.* (1981). The broken line shows the 3σ total uncertainty in the present results.

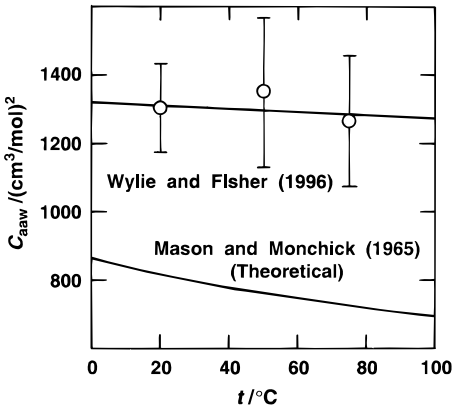

Figure 6. Present results for C_{aaw} and the theoretical results of Mason and Monchick (1965). The error bars show the 3σ total uncertainties calculated independently for each temperature.

estimates of Mason and Monchick (1965) and Chaddock (1965).

As the Goff measurements, for temperatures from 5 to 25 °C, were restricted to pressures of a few atmospheres so that the interaction third virial coefficients, unknown at the time, could be neglected, it is remarkable that those researchers achieved even the accuracy apparent in Figure 4. Their results agree with ours within their implied 3σ uncertainty.

Wexler *et al.* (1981) later collated all the NBS results for B_{aw}, our 1974 results, and our early results for 75 °C (privately communicated), and included the resulting values in an extensive tabulation of derived system properties (Wexler *et al.*, 1981). Figure 5 shows the differences of the respective NBS data and of this collation from the present results. Hyland's collation differs from the present results by 2.0 times the present uncertainty at 0 °C but becomes equal at about 110 °C. The collation of Wexler *et al.* (1981) differs by 2.6 times the present uncertainty at 0 °C, becoming equal near 80 °C.

Both the theoretical estimates of $B_{aw}(T)$ were made using L-J (6−12) potentials, and using rules to combine the two parameters of the air−air potential with the appropriate parameters of the water−water potential. However, while Mason and Monchick used the simplest form of the largely empirical combining rules, Chaddock used a form with more regard for the permanent dipole moment of the water molecule. Figure 4 shows that neither of these simple methods gives a good estimate.

The only earlier values of C_{aaw} are those obtained theoretically by Mason and Monchick (1965) using the combining procedure of Rowlinson *et al.* (1954). They are plotted in Figure 6 along with the present values, from which they differ by several times the present uncertainty. However, the difference is embraced by the rather tentative estimate of an uncertainty of a factor of 2 given by those authors. The Mason and Monchick estimate of C_{aaw}, being all that was available, has been used by Wexler and Hyland in all their work.

Some Further Considerations. The present data for B_{aw} are comparable in uncertainty with the best data available for self second virial coefficients. The data for C_{aaw} are the only experimental data available. Except for low pressures, the correlations between the uncertainties in the respective terms are likely to mean that the accuracy of calculations of f_w, g_w, or other thermodynamic properties would be impaired if data for B_{aw}, C_{aaw}, or C_{aww} from other sources were brought in. This would be likely to remain true even if a much better estimate of C_{aww} became

available, unless the present experimental results were reanalyzed to give slightly modified values of B_{aw} and C_{aaw}.

The density series for W (eq 8) can be inverted to a pressure series. Sample calculations have shown that if only the second and third virial coefficients of the density expansion are retained, and W is inverted to the pressure form, it is necessary for the present purposes to retain terms as far as that in p^6 to preserve the accuracy. Thus, at least in the present context, the density series converges much more rapidly than the pressure series.

Literature Cited

Chaddock, J. B. Moist Air Properties from Tabulated Virial Coefficients. *Humidity and Moisture*, Reinhold: New York, 1965; Vol. 3, pp 273−284.

Ewald, A. H.; Jepson, W. B.; Rowlinson, J. S. The Solubility of Solids in Gases. *Discuss. Faraday Soc.* **1953**, No. 15, 238−243.

Goff, J. A. Final Report of the Working Subcommittee of the International Joint Committee on Psychrometric Data. *Trans. ASME* **1949**, *71*, 903−913.

Goff, J. A.; Gratch, S. Thermodynamic Properties of Moist Air. *Heat./Piping/Air Cond. (ASHVE J. Sect.)* **1945**, *17*, 334−348.

Handbook of Chemistry, 10th ed.; Lange, N. A., Ed.; McGraw-Hill: New York, 1961; pp 268−269.

Handbook of Chemistry and Physics, 72nd ed.; CRC Press: Boca Raton, FL 1991−92; Section 4, p 71.

Harrison, L. P. Fundamental Concepts and Definitions Relating to Humidity. *Humidity and Moisture*; Reinhold: New York, 1965; Vol. 3, pp 3−69.

Himmelblau, D. M. Solubilities of Inert Gases in H_2O: 0° to near the Critical Point of H_2O. *J. Chem. Eng. Data* **1960**, *5*, 10−15.

Hirschfelder, J. O.; Curtiss, C. F.; Bird, R. B. *Molecular Theory of Gases and Liquids*; Wiley: New York, 1964.

Holborn, L.; Otto, J. On the Isotherms of a Gas between +400 and −183 °C. *Z. Phys.* **1925**, *33*, 1−11.

Hyland, R. W. A Correlation for the Second Interaction Virial Coefficients and Enhancement Factors for Moist Air. *J. Res. Natl. Bur. Stand. (U.S.)* **1975**, *A79*, 551−560.

Hyland, R. W.; Mason, E. A. Corrections to Paper Entitled "Third Virial Coefficient for Air-Water Vapour Mixtures". *J. Res. Natl. Bur. Stand. (U.S.)* **1975**, *A79*, 775−776.

Hyland, R. W.; Wexler, A. The Enhancement of Water Vapour in Carbon Dioxide-Free Air at 30, 40 and 50 °C. *J. Res. Natl. Bur. Stand. (U.S.)* **1973**, *A77*, 115−131; v. also *A77*, 133−147.

Kell, G. S. Density, Thermal Expansivity, and Compressibility of Liquid Water from 0° to 150 °C: Correlations and Tables for Atmospheric Pressure and Saturation Reviewed and Expressed on 1968 Temperature Scale. *J. Chem. Eng. Data* **1975**, *20*, 97−105.

Kell, G. S.; Whalley, E. The PVT Properties of Water. I. Liquid Water in the Temperature Range 0 to 150 °C and at Pressures up to 1 kb. *Philos Trans. R. Soc. London, A.* **1965**, *258*, 565−614.

Maitland, G. C.; Rigby, M.; Smith, E. B.; Wakeham, W. A. *Intermolecular Forces*: *Their Origin and Determination*; Clarendon: Oxford, 1981; p 133; see also their ref 2, p 253.

Mason, E. A.; Monchick, L. Survey of the Equation of State and Transport Properties of Moist Gases. *Humidity and Moisture*; Reinhold: New York, 1965; Vol. 3, pp 257−272.

Mason, E. A.; Spurling, T. H. *The Virial Equation of State*; Pergamon: Oxford, 1969; p 111.

Mayer, J. E. Statistical Mechanics of Condensing Systems. V. Two-Component Systems. *J. Phys. Chem.* **1939**, *43*, 71−95.

Michels, A.; Wassenaar, T.; van Seventer, W. Isotherms of Air between 0 °C and 75 °C and at Pressures up to 2200 ATM. *Appl. Sci. Res.* **1953**, *A4*, 52−56.

Pollitzer, F.; Strebel, E. On the Influence of an Indifferent Gas on the Concentration of the Saturated Vapour of Liquids. *Z. Phys. Chem.* **1924**, *110*, 768−785.

Preston-Thomas, H. The International Temperature Scale of 1990 (ITS-90). *Metrologia* **1990**, *27*, 3−10, 107.

Rowlinson, J. S.; Richardson, M. J. The Solubility of Solids in Compressed Gases. *Adv. Chem. Phys.* **1959**, *2*, 85−118.

Rowlinson, J. S.; Sumner, F. H.; Sutton, J. R. The Virial Coefficients of a Gas Mixture. *Trans. Faraday Soc.* **1954**, *50*, 1−8.

Thompson, A. M.; Small, G. W. A.C. Bridge for Platinum-Resistance Thermometry. *Proc. Inst. Electr. Eng.* **1971**, *118*, 1662−1666.

Webster, T. J. The Effect on Water Vapour Pressure of Superimposed Air Pressure. *J. Soc. Chem. Ind., London* **1950**, *69*, 343−346.

Wexler, A. Vapour Pressure Formulation for Water in Range 0 to 100 °C. A Revision. *J. Res. Natl. Bur. Stand. (U.S.)* **1976**, *A80*, 775−785.

Wexler, A.; Hyland, R.; Stewart, R. *Thermodynamic Properties of Dry Air, Moist Air and Water and SI Psychrometric Charts*; ASHRAE: Atlanta, 1981.

Wiebe, R.; Gaddy, V. L.; Heins, C. Jr. The Solubility of Nitrogen in Water at 50°, 75° and 100 °C from 25 to 1000 Atmospheres. *J. Am. Chem. Soc.* **1933**, *55*, 947−953.

Wylie, R. G. A New Absolute Method of Hygrometry. *Aust. J. Phys.* **1957**, *10*, 351−365, 429−453.

Wylie, R. G.; Fisher, R. S. Accurate Determination of the Molecular Interaction in a Gas-Vapour Mixture. *Fifth Convention of the Royal Australian Chemical Institute, Canberra, May 1974, Physical Chemistry Section*; RACI: Melbourne, 1974.

Zoss, L. M.; Suciu, S. N.; Sibbitt, W. L. The Solubility of Oxygen in Water. *Trans. ASME* **1954**, *76*, 69−71.

Received for review April 20, 1995. Accepted October 21, 1995.[⊗]

JE950092L

[⊗] Abstract published in *Advance ACS Abstracts*, December 1, 1995.